RSC Sustainability

ROYAL SOCIETY OF CHEMISTRY

PAPER

View Article Online
View Journal

Cite this: DOI: 10.1039/d6su00050a

Energy utilization strategies in lignocellulosic biorefineries

Emmanuel A. Aboagye [a] and Christos T. Maravelias *[ab]

Lignocellulosic biorefineries can generate various energy-rich side streams, including biogas from anaerobic digestion, a lignin stream from biomass pretreatment, and conversion residues. This study evaluates different chemical energy utilization strategies in lignocellulosic biorefineries based on energy and carbon efficiencies, cost, and greenhouse gas mitigation potential. Specifically, using modeling and optimization, we examine strategies that include electricity generation, biogas upgrade to biomethane, lignin valorization, and carbon capture and storage. We find that upgrading biogas to biomethane demonstrates the highest energy efficiency and leads to the lowest minimum fuel selling price for the main product, ethanol. The biorefinery with carbon capture and storage achieves the lowest net carbon footprint. Lignin valorization has the highest carbon footprint due to the additional materials required for lignin depolymerization, despite its potential to produce high value bioproducts.

Received 26th January 2026
Accepted 12th March 2026

DOI: 10.1039/d6su00050a

rsc.li/rscsus

Sustainability spotlight

Lignocellulosic biorefineries are expected to play a pivotal role in achieving net-zero emissions. In addition to producing liquid fuels, biorefineries have energy-rich side streams (lignin, biogas, and conversion residues) which can also be converted to valuable co-products. In that respect, a central question is how these side streams should be utilized to balance economic and environmental performance. While most studies have focused on electricity co-production, alternative strategies like biomethane production, lignin valorization, and carbon capture and storage may offer superior outcomes. Accordingly, this system-level study analyzes the energy and carbon flows, as well as economic and environmental impacts of different lignocellulosic biorefineries, to understand the major trade-offs and derive key insights that can inform the adoption of lignocellulosic biofuels.

1 Introduction

The adoption and development of second-generation lignocellulosic biorefineries[1–3] can play a critical role towards a sustainable energy future.[4] Lignocellulosic biorefineries not only offer a renewable and reliable source of bioenergy but also contribute to greenhouse gas (GHG) reduction,[5–7] energy security,[8] and can drive economic growth.[9] The majority of system-level studies focus on converting excess chemical energy from side streams (*e.g.*, lignin, biogas from anaerobic digestion, wastewater sludge, and conversion residue) into a single co-product, typically electricity.[10–14] These studies have demonstrated that co-producing electricity can enhance overall energy efficiency and help displace fossil-based grid emissions. Although, this approach offers a straightforward means to utilize surplus energy, generate additional revenue, and integrate renewable energy into existing power infrastructure, it may not necessarily constitute the best way of utilizing these energy-rich side streams. Alternative strategies may lead to systems that are economically more attractive and more sustainable.

Upgrading biogas to biomethane[1,15–17] is one such alternative. Biomethane, a renewable fuel, can be directly injected into natural gas pipelines. However, research on capturing and upgrading biogas to biomethane in second-generation biorefinery design remains limited. Lignin valorization[18–21] is another promising alternative, with considerable research focused on studying various technologies and products, placing special emphasis on advancing catalytic approaches[20,22,23] to enhance key economic drivers.[24,25] Utilizing the surplus chemical energy in the side streams for heat generation further enables the integration of carbon capture and storage (CCS),[26–28] which can significantly reduce GHG emissions.[11,27,29]

While these strategies have been proposed, it remains unclear which one is the best in terms of economic viability, environmental sustainability, and overall system performance; as well as under what incentive structure. Furthermore, it is unclear how the use of natural gas for CO_2 capture impacts the economic potential and fossil-based emissions of biorefineries. Additionally, the impact of numerous factors, such as renewable energy and fuel incentives, CO_2 sequestration credits, energy demand of co-product technologies, and co-product selling prices is not fully understood.

[a]*Department of Chemical and Biological Engineering, Princeton University, Princeton, NJ, USA. E-mail: maravelias@princeton.edu*

[b]*Andlinger Center for Energy and the Environment, Princeton University, Princeton, NJ, USA*

Accordingly, the goal of this study is to assess and compare different lignocellulosic biorefinery strategies, identify key drivers, evaluate trade-offs, and draw insights into system performance. We study three co-production baseline systems: (1) surplus electricity generation, (2) upgrading biogas to biomethane, and (3) valorizing lignin into high value bioproduct. We examine carbon and energy flows, economic potential, carbon footprint (CF), as well as overall energy efficiency of these baseline systems. We then study a biorefinery with carbon capture and sequestration and subsequently explore the implications of natural gas usage. We extend the scope of our study to investigate the impacts of key parameters on system economics and CF, and further explore options for CO_2 mitigation by integrating carbon capture in the three baseline systems. Finally, we extend the work for the electricity and biomethane baseline systems to assess how geographic variability in co-product selling price could influence, potentially, the preferred biorefinery systems across the contiguous United States (U.S.).

2 Methods

In this section, we present the co-production baseline systems, the CCS system, and the integrated (co-production and CCS) systems. We then discuss key data, assumptions, and the optimization model used for the analysis. We represent each biorefinery using the Latin letter "B" with a subscript denoting the co-product ("EL" – electricity, "BM" – biomethane, "LV" – lignin valorization), and a superscript indicating the presence of CCS. In biorefineries where we have CCS integrated with co-production, additional energy may be required, hence we use a preceding "+" to signify that natural gas and electricity purchases are allowed. Thus, the general representation is given as $+B^{CCS}_{\{EL,BM,LV\}}$. The abbreviations of the biorefinery systems are as follows:

- B_{EL}: biorefinery with electricity co-production.
- B_{BM}: biorefinery with biomethane co-production.
- B_{LV}: biorefinery with biochemical co-production *via* lignin valorization.
- B^{CCS}: biorefinery with carbon capture and storage.
- $+B^{CCS}_{EL}$: integrated biorefinery with electricity co-production and carbon capture and storage.
- $+B^{CCS}_{BM}$: integrated biorefinery with biomethane co-production and carbon capture and storage.
- $+B^{CCS}_{LV}$: integrated biorefinery with lignin valorization and carbon capture and storage.

2.1 Biorefinery systems description

To ensure consistency and derive insights applicable across all biorefineries, we use the following subsystem in all baselines: biomass undergoes pretreatment, followed by enzymatic hydrolysis to convert carbohydrates into sugars which are fermented to produce ethanol with the release of CO_2; ethanol is recovered as fuel while the residual stream is separated into stillage and lignin; biogas consisting of 73 wt% CO_2 and 23 wt% CH_4 is produced from the stillage through anaerobic digestion.

In the B_{EL} system, all side streams (lignin, biogas, wastewater sludge, conversion residue) are combusted to generate heat and electricity with excess electricity sold to the grid (Fig. 1a). In the B_{BM} system (Fig. 1b), a fraction of CH_4 is recovered from the biogas stream to produce biomethane, while the CO_2 stream is vented. The remaining biogas, wastewater sludge, and the lignin streams are used to meet biorefinery energy requirements. In the B_{LV} system (Fig. 1c), a fraction of the lignin stream is converted into valuable biochemical. We use acetic acid as a model compound to represent lignin valorization. In the B^{CCS} system (Fig. 1d), we have the option to capture CO_2 from the fermentation CO_2-containing stream (~95 wt%), biogas (73 wt% CO_2, 23 wt% CH_4), and post-combustion flue gas (~20 wt%). If CO_2 from biogas is captured, the remaining methane is combusted.

In all the integrated systems ($+B^{CCS}_{EL}$, $+B^{CCS}_{BM}$, and $+B^{CCS}_{LV}$), we can capture CO_2 from the gas outlet of fermentation and flue gas. However, in the $+B^{CCS}_{BM}$ system, CO_2 resulting from biomethane recovery can also be captured (see Fig. 1 in SI for details).

2.2 Basis, data, and assumptions

In all analyses, we express results for producing 1 kg of biofuel from corn stover (dry basis). Corn stover is selected as a representative lignocellulosic feedstock due to its extensive characterization in the literature and relevance to U.S. biorefinery deployment; results should therefore be interpreted as benchmark comparisons rather than universal feedstock-agnostic values, though we expect that the qualitative findings of this study to be valid across lignocellulosic feedstocks. Process and economic data are sourced from NREL reports,[10,13,30,31] while emission factors for CF analysis are from the US Life Cycle Inventory[32] database. The composition of corn stover is provided in Table S1. Conversion data for components, auxiliary material consumption, lower heating values, and other process related parameters are detailed in Tables S2–S5. We assume an acetic acid yield of 0.39 kg per kg of lignin feedstock.[33,34] The energy demand for each block is listed in Table S6. The chemical-to-heat conversion in the combustor has 80% efficiency,[13] while the heat-to-electricity efficiency in the turbogenerator is 40% (ref. 35) with 50% heat recovery.[35]

Feedstock and utility prices, financial incentives, and other economic related data can be found in Table S5, while Table S6 contains block production cost (see Note S1 for production cost explanation). For the analysis of spatial specificity, state-level co-product selling price and emission factor can be found in Table S7. Other emission factors are listed in Table S8. For electricity, the average emission factor of the US grid is assumed (107 g CO_2e per MJ). We assume that corn stover is a byproduct of corn farming and exclude soil organic carbon sequestration in CF analysis. Biogenic CO_2 emissions are assumed to be carbon neutral. Pressure swing adsorption and monoethanolamine absorption are used for CO_2 capture from biogas and flue gas streams, respectively with efficiencies of 98% and 85%, respectively.[36,37]

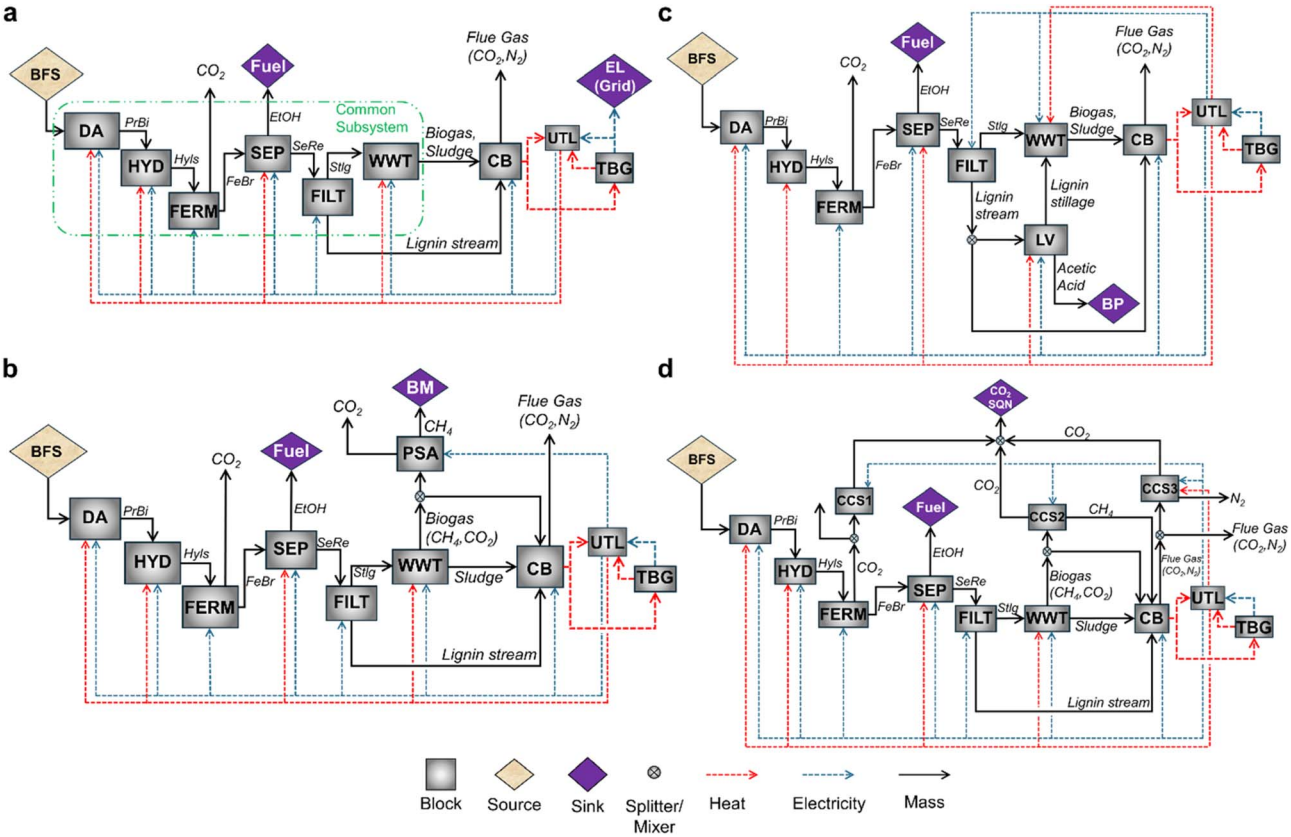

Fig. 1 Block flow diagram of the three co-production baseline systems, and the carbon capture system. (a) B_{EL}, (b) B_{BM}, (c) B_{LV} and (d) B^{CCS}. Abbreviations: DA: dilute acid, HYD: hydrolysis, FERM: fermentation, SEP: separation, FILT: filtration, WWT: wastewater treatment, CB: combustor, TBG: turbogenerator, UTL: utility, CCS: carbon capture and storage, LV: lignin valorization, PSA: pressure swing adsorption, SQN: sequestration, BM: biomethane, BP: bioproduct, EL: electricity, BFS: biomass feedstock, PrBi: pretreated biomass, Hyls: hydrolysate, FeBr: fermentation broth, EtOH: ethanol, SeRe: separation residual, Stlg: stillage.

2.3 Process modeling

Detailed mathematical equations and conventions are provided in the SI Methods, with some main equations presented here. Variables are denoted by italicized Latin letters, with a superscript indicating different features associated with the system. We develop mixed-integer nonlinear programming (MINLP) models to minimize the total cost, C as indicated by eqn (1). This cost represents the minimum fuel selling price (MFSP) needed so that the total revenue from selling the biofuel and other products equals the total costs, that is, it is at breakeven price.

$$C = C^{FES} + C^{TRN} + C^{PRD} + C^{UTL} + C^{SEQ} - R^{COP} - R^{CSS} \quad (1)$$

The developed models consist of material and energy balances, economic and CF calculations, and constraints. We use binary variables for block selection and for logical restrictions (*e.g.*, if we sell electricity to the grid, then we cannot purchase grid electricity), while continuous variables are used for material, energy, and cash flows.

The total cost consists of feedstock (C^{FES}), feedstock transportation (C^{TRN}), production (C^{PRD}), utility (C^{UTL}, natural gas or electricity purchase), and sequestration (C^{SEQ}) costs. These are offset by revenue from co-product sales and incentives (R^{COP}), and carbon capture credits (R^{CSS}). Production cost entails capital and operating costs. Sequestration cost includes transportation to the geological site, and the sequestration process, while CO_2 capture costs are incorporated into production costs. Co-product incentives include renewable energy credits (RECs),[38] clean fuel production credit (CFPC)[39] and renewable identification number (D3-RIN under the renewable fuel standard program).[40]

We calculate the net CF, G for each biorefinery using eqn (2). This accounts for all direct and indirect emissions of the biorefinery, G^{BRN} including feedstock handling, transportation, auxiliary material consumption in the biorefinery, and natural gas and electricity usage. To estimate the net CF, we subtract the displaced emissions due to co-product production (G^{DIP}), and the amount of carbon captured by systems with carbon capture options (G^{CCS}), from the biorefinery direct and indirect emissions. We report the results associated with CF in grams of carbon dioxide equivalent per megajoule of ethanol (g CO_2e per MJ), unless otherwise stated.

$$G = G^{BRN} - G^{DIP} - G^{CCS} \quad (2)$$

When we compare the economic viability, with and without natural gas purchase, in the carbon capture system, we employ the marginal abatement cost metric[41] which is an economic indicator used to assess the additional cost of mitigating a unit mass of GHG emission when a different emission reduction strategy is used. In the integrated systems where we implement emission constraint for CO_2 mitigation, we use eqn (3) for different values of epsilon (ε).

$$G \leq \varepsilon \tag{3}$$

Finally, we use ${}^{NG}_{EL}\mathrm{C}^{\mathrm{CCS}.\{1,2,3\}}_{\{\mathrm{EL,BM,LV}\}}$ to denote the system configuration in a solution shown in figures. Here, "C" represents a system configuration based on the model solution, "NG" and "EL" are used to imply whether natural gas and electricity are purchased, while numbers 1–3 represent the CCS capture options ("1" – fermentation CO_2, "2" – biogas CO_2, "3" – flue gas CO_2).

3 Results

In the following sections, we present the analysis for the co-production baseline systems, examine the carbon capture system, and present the analysis of the various extensions to the baselines, with all results interpreted within a consistent comparative framework to evaluate performance across systems under identical sub-system modeling assumptions.

3.1 Co-production baselines

Producing 1 kg of biofuel (26.8 MJ of ethanol) requires 3.94 kg of biomass (63.9 MJ) of corn stover, with 42% of the total chemical energy converted to biofuel, and 27.2 MJ (55% lignin, 36% biogas, 3% glucan, 3% wastewater sludge, 1% xylan) available for different utilization strategies.

The B_{EL} system (Fig. 2a) uses all 27.2 MJ for heat generation, resulting in 21.8 MJ of heat produced. Here, 1.1 MJ of the generated heat is initially used for heating, while the remaining 95% is sent to the turbogenerator to maximize electricity production. This results in 5.8 MJ of electricity being sold to the grid, indicating that ~0.22 MJ of renewable energy can be generated per MJ of biofuel produced.

Fig. 2b illustrates the B_{BM} system where 18.9 MJ is used for heat and power generation and 8.3 MJ is upgraded to biomethane. Notably, the pressure swing adsorption employed for the upgrade, which requires only electricity, consumes ~17% of the electricity generated. If an alternative upgrading technology requiring both heat and electricity is employed, a reduced amount of biomethane would be produced because additional heat would need to be sourced from the biogas that is upgraded (see Fig. S2 for such analysis).

In the B_{LV} system (Fig. 2c), 72% (wt) of the lignin stream, which corresponds to 11.6 MJ, is used for valorization with the rest combusted. The portion of the lignin stream that can be valorized into bioproduct, from an energy perspective, depends

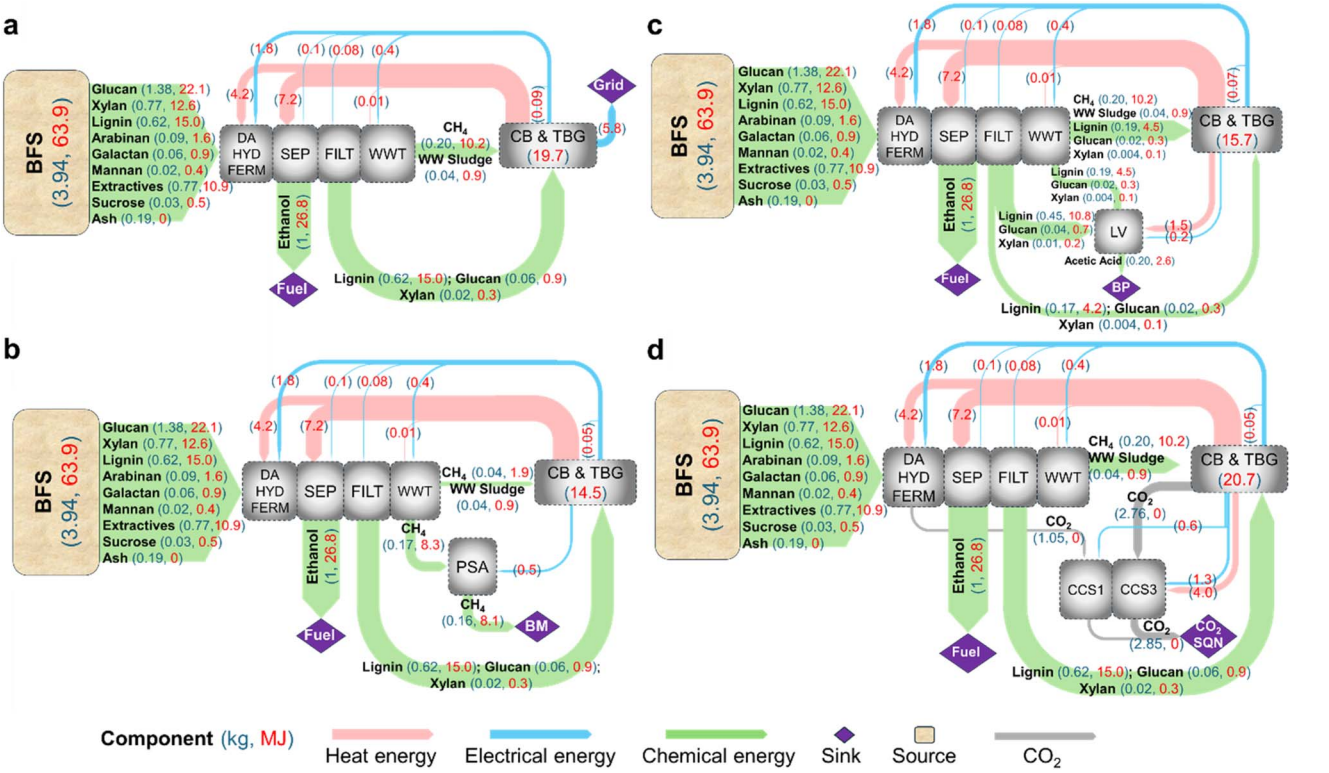

Fig. 2 Energy and mass flows of the three co-production baseline systems, and the carbon capture system. (a) B_{EL}, (b) B_{BM}, (c) B_{LV} and (d) B^{CCS}. Abbreviations: DA: dilute acid, HYD: hydrolysis, FERM: fermentation, SEP: separator, FILT: filtration, WWT: wastewater treatment, CB: combustor, TBG: turbogenerator, PSA: pressure swing adsorption, LV: lignin valorization, CCS: carbon capture and storage, BM: biomethane, BP: bioproduct, SQN: sequestration, BFS: biomass feedstock.

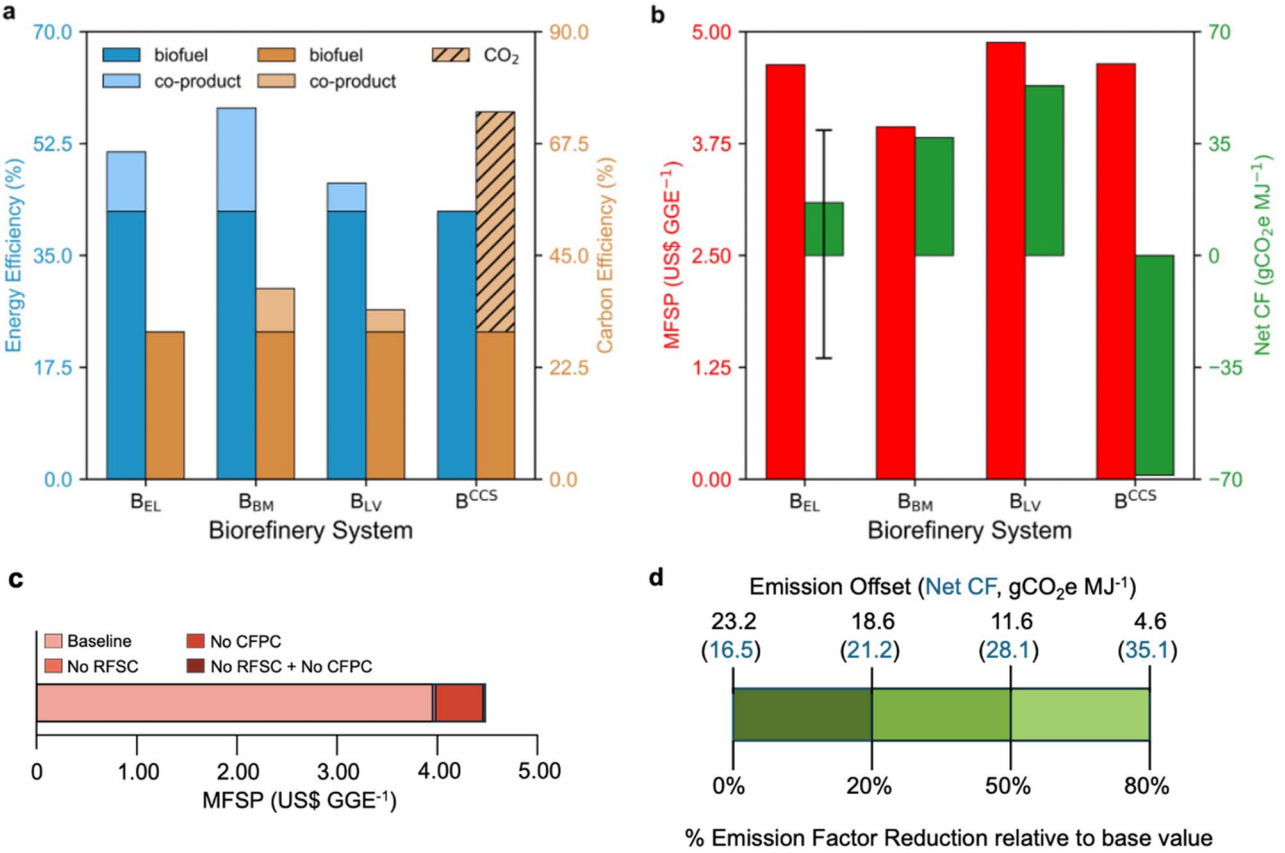

Fig. 3 Key metrics of the three co-production baseline systems, and the carbon capture system. (a) Energy and carbon efficiencies; determined by dividing the energy and carbon contents of the fuel and co-product by the corresponding energy and carbon contents in the biomass. (b) MFSP and net CF; the "whisker" in the net CF of the B_{EL} system represent scenarios where electricity sold offsets emission from four different power sources; the "excess" amount of emission offset relative to the baseline are 48.7, 17.9, −22.7, 46.8 g CO_2e per MJ, for coal, natural gas, nuclear, and diesel power plants, respectively. (c) Sequential, changes in MFSP of the B_{BM} system resulting from the removal of D3-RINs, CFPC, and both incentives, read cumulatively from the baseline value. (d) Impact of emission factor reduction (improvement in grid carbon intensity) on carbon footprint for the B_{EL} system.

primarily on the energy requirements of the valorization block (see Fig. S3a–d for water flows).

The B_{BM} system has the highest energy efficiency (58%) due to the higher specific energy of biomethane, while the B_{LV} has the lowest (Fig. 3a). From a carbon efficiency standpoint, the B_{BM} has the highest (38%) whereas B_{EL} has the lowest (Fig. 3a). All systems have ∼8% carbon losses, primarily in the pretreatment and hydrolysis blocks. However, the B_{LV} system incurs additional losses (∼7%) in the valorization block (see Fig. S3 for carbon flows).

3.2 Co-product revenue

In the B_{EL} system, the additional benefit from selling electricity includes revenue from RECs (US$1 per MWh was used), which results in a MFSP of US$4.63 per GGE (Fig. 3b). Assuming an upper bound of US$35 per MWh on RECs decreases the MFSP by 5%. The B_{BM} has the lowest MFSP at US$3.94 per GGE (Fig. 3b). The additional benefits from biomethane sales include the D3-RIN and the CFPC (US$0.05 per gal and US$0.20 per gal were used, respectively). Applying the upper bound for each incentive reduces the MFSP by 50% (US$1.97 per GGE). In the absence of the D3-RIN, CFPC, or both, the MFSP increases from the baseline value to US$3.97, US$4.45, and US$4.47 per GGE, respectively (Fig. 3c). In the B_{LV} system (Fig. 3b), revenue comes from acetic acid sales. This results in a MFSP of US$4.86 per GGE (see Fig. S4a for MFSP breakdown of each system).

3.3 Co-product emission offset

From a sustainability perspective (Fig. 3b), the B_{EL} exhibits the lowest CF, with a net value of 16.5 g CO_2e per MJ, followed by B_{BM} (36.9 g CO_2e per MJ) and B_{LV} systems (53.1 g CO_2e per MJ). The B_{EL} offsets approximately 23.2 g CO_2e per MJ of emissions (based on the average emission factor of the US electricity grid). However, as the carbon intensity of the electricity grid declines due to increased penetration of renewables, the emissions offset due to surplus electricity decreases (from 23.2 to 4.6 g CO_2e per MJ), increasing the carbon footprint of the B_{EL} system (Fig. 3d). Additionally, if electricity sales result in emission offset from different power sources, the amount displaced, and consequently the net CF, would vary as indicated by the black vertical line in the B_{EL} net CF figure. Producing biomethane enables 2.8 g CO_2e per MJ offset, while 11.6 g CO_2e per MJ is

displaced for acetic acid production. However, the high net CF of the B_{LV} system is due to the auxiliary chemicals needed for lignin depolymerization (see net CF breakdown in Fig. S4b).

3.4 Carbon capture system

Fig. 2d shows the B^{CCS} system where all CO_2 from the fermentation is captured while the biogas stream is combusted, leading to the capture of 55% of the CO_2 from flue gas. The system generates 20.7 MJ of heat and power with 29% used for capture. The energy and carbon efficiencies are 42% and 30%, respectively (Fig. 3a). However, if we consider the carbon captured, the carbon efficiency increases to 73%. We use a credit of US$85 per Mg, given to facilities that capture and store CO_2 in the US which translate to a MFSP of US$4.64 per GGE (Fig. 3b), with a net CF of −68.7 g CO_2e per MJ and 106.2 g CO_2 per MJ captured (see Fig. S4 and S5 for MFSP and CF breakdown, and carbon flow). If natural gas is purchased for carbon capture, the captured CO_2 increases to 135.3 g CO_2 per MJ, requiring 0.059 kg of natural gas. However, the MFSP increases by 4% with a net CF of −96.8 g CO_2e per MJ (see Fig. S6 for breakdown). This translates to a calculated marginal abatement cost of US$55 per Mg of CO_2 captured.

3.5 Co-product selling price and production costs

Price fluctuations could significantly influence biorefinery economic viability. For example, in 2022, U.S. electricity prices[42] varied, from US$0.07 to US$0.25 per kWh, while biomethane prices ranged between US$0.14 and US$1.45 per kg, with acetic acid prices[43] ranging between $0.63 and $0.87 per kg. Therefore, we assess how co-product selling price and their block production cost impact each baseline system. In this analysis, we allow electricity and natural gas purchases when internal energy supply is insufficient to meet heating and power demands. These purchases, however, introduce emissions.

In the $+B_{EL}$ system (Fig. 4a and d), lower production costs and higher selling prices lead to about 0.03 kg of natural gas purchase and increased electricity sales (from 5.8 MJ to 6.7 MJ), resulting in a reduced MFSP. Contrary to expectations, the net CF is not the highest with natural gas purchase. While the purchase of 0.03 kg of natural gas contributes 0.52 g CO_2e per MJ to CF, the sale of electricity contributes −26.8 g CO_2e per MJ, yielding a net reduction of −26.3 g CO_2e per MJ. At higher production costs and lower selling prices, natural gas is not purchased, and the biorefinery reverts to the baseline B_{EL} with 5.8 MJ of electricity sold, leading to a net reduction of −23.2 g CO_2e per MJ, and hence higher net CF.

In the $+B_{BM}$ system (Fig. 4b and e), when production costs are high and selling prices are low, 82% of the biogas stream is allocated to biomethane production and the rest is used for energy generation, resulting in a lower CF, but higher MFSP. As production cost decreases and selling price increases, the entire biogas stream is used for biomethane production, necessitating grid electricity purchase. This reduces the MFSP but increases the net CF.

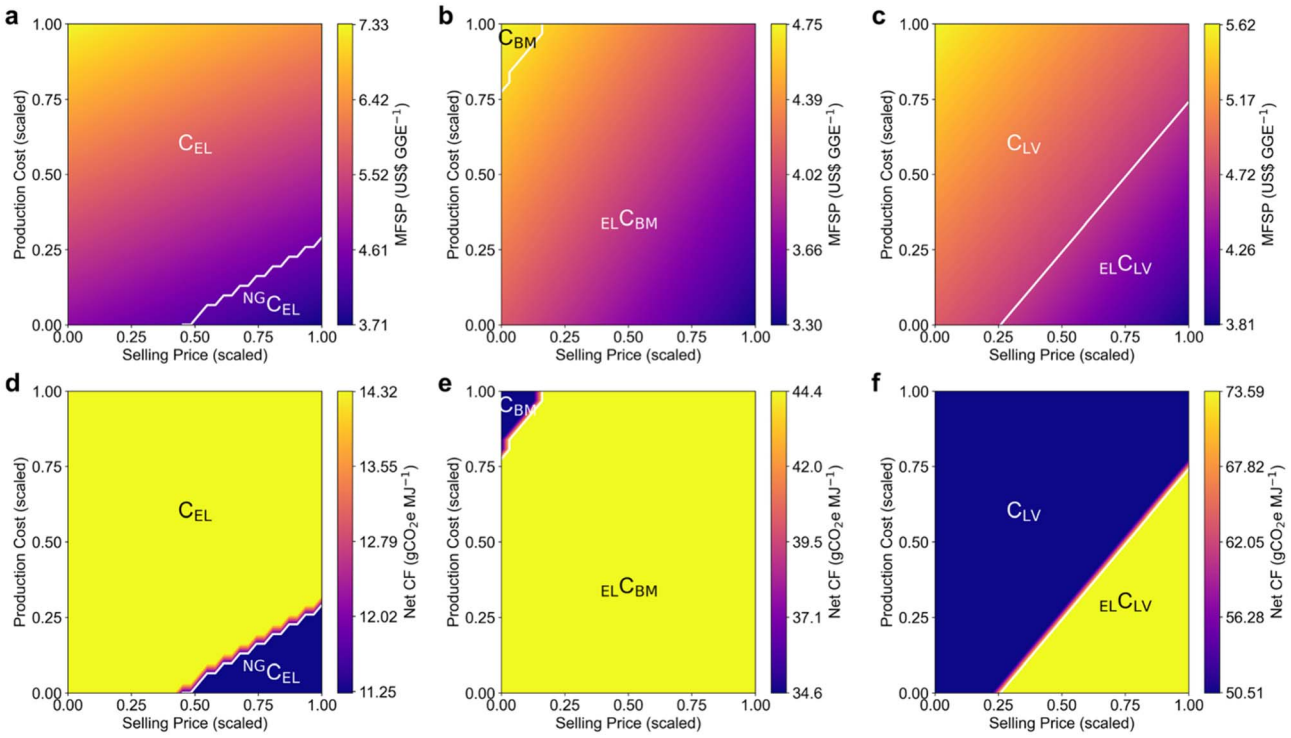

Fig. 4 MFSP and CF of co-production systems as a function of co-product selling price and corresponding block production cost. (a and d) $+B_{EL}$ system, production cost of turbogenerator block: 0.001–0.1 US$ per kWh, selling price of electricity: 0.02–0.15 US$ per kWh. (b and e) $+B_{BM}$ system, production cost of pressure swing adsorption block: 0.01–0.2 US$ per kg, selling price of biomethane: 0.1–1.0 US$ per kg. (c and f) $+B_{LV}$ system, production cost of lignin valorization: 0.01–0.35 US$ per kg, selling price of acetic acid: 0.1–1.0 US$ per kg.

At higher production costs and lower selling prices for the $+B_{LV}$ system (Fig. 4c and f), 72% of the lignin stream is valorized, with electricity (2.7 MJ) generated by the biorefinery, hence lower net CF, but higher MFSP. However, at lower production costs and higher selling prices, all the lignin stream is valorized, leading to electricity purchase (2.3 MJ) to meet the electricity demand. This results in a lower MFSP but higher net CF.

3.6 CO_2 mitigation strategies in co-production systems

We examine CO_2 mitigation strategies in the co-production baselines by integrating carbon capture in each system. We explore two approaches: (1) vary sequestration credits and (2) enforce emission constraints. Electricity and natural gas purchases are allowed.

Fig. 5a shows how sequestration credits impact the MFSP, amount of CO_2 captured, net CF, and amount of external energy purchased. At lower credits, we capture no CO_2, leading to higher CF and MFSP in all systems. In $+B_{EL}^{CCS}$, we begin capturing fermentation CO_2 at US$51.5 per Mg, reducing electricity sales from 5.8 MJ to 5.4 MJ. At US$106 per Mg, maximum CO_2 capture from flue gas stream makes capturing financially more attractive than selling electricity. In $+B_{BM}^{CCS}$, we similarly start capturing at US$51.5 per Mg from both fermentation and the biogas separation. This increases electricity purchases from 1.3 MJ to 2.2 MJ. At US$106 per Mg, we capture 47% of flue gas CO_2, necessitating 4.4 MJ of electricity purchase. To capture the maximum CO_2 from flue gas stream, credits must be around US$127 per Mg. In $+B_{LV}^{CCS}$, we start to capture CO_2 from fermentation at US$46.9 per Mg as the fraction of lignin that is valorized decreases from 72% to 65% to account for needed electricity. At US$81.8 per Mg, 65% CO_2 capture from flue gas requires burning the entire lignin stream, and at US$106 per Mg, maximum CO_2 capture necessitates purchase of electricity. Both $+B_{EL}^{CCS}$ and $+B_{LV}^{CCS}$ achieve similar CF and CO_2 capture at credits above US$106 per Mg by trading-off co-product production for carbon capture and hence have the same trend of imported energy.

Next, we fix the sequestration credits at US$85 per Mg, and we impose emission constraints using targeted reduction values (epsilon) to gain deeper insight into CO_2 mitigation strategies. From Fig. 5b, we observe that at more stringent emission constraints all three systems exhibit higher costs. At −107.4 g CO_2e per MJ, all systems capture the maximum possible CO_2 from fermentation, and flue gas (and from biogas for $+B_{BM}^{CCS}$ system) with the purchase of natural gas and electricity. Once the constraint is relaxed, the MFSP starts to reduce gradually. We observe that between −100 g CO_2e per MJ and −50 g CO_2e per MJ, it is possible to reduce emission by a factor of 2 for ∼14% increase in cost.

4 Discussion

Building upon the analysis presented so far, we derive additional critical insights to further inform future biorefinery deployment.

4.1 Further insights

One of the important aspects to examine, from the energy utilization perspective, is the total energy consumed (heat and electricity) to make biofuel and co-product, and the primary energy content of co-product per kg of biomass feedstock processed. Focusing on the three baselines, Fig. 6a indicates that the B_{LV} system has the highest specific energy consumption. Furthermore, the B_{BM} system has the highest primary energy content of co-product per kg of biomass feedstock (∼2.0 MJ kg^{-1}, Fig. 6a), with the B_{LV} having the lowest value of ∼0.7 MJ kg^{-1}. In Fig. 6b, we observe relatively similar revenue per kg of biomass feedstock for both B_{EL} and B_{LV}. However, this observation could change depending on the target chemical for lignin valorization. Additionally, the B_{LV} system appears to currently have the highest production cost.

In the B^{CCS} system, the specific energy consumption is ∼5.3 MJ kg^{-1} (Fig. 6a), and the main option for energy consumption reduction is to improve the capturing efficiency of technologies at lower energy demand for, mainly, flue gas CO_2. In Fig. 6b, we

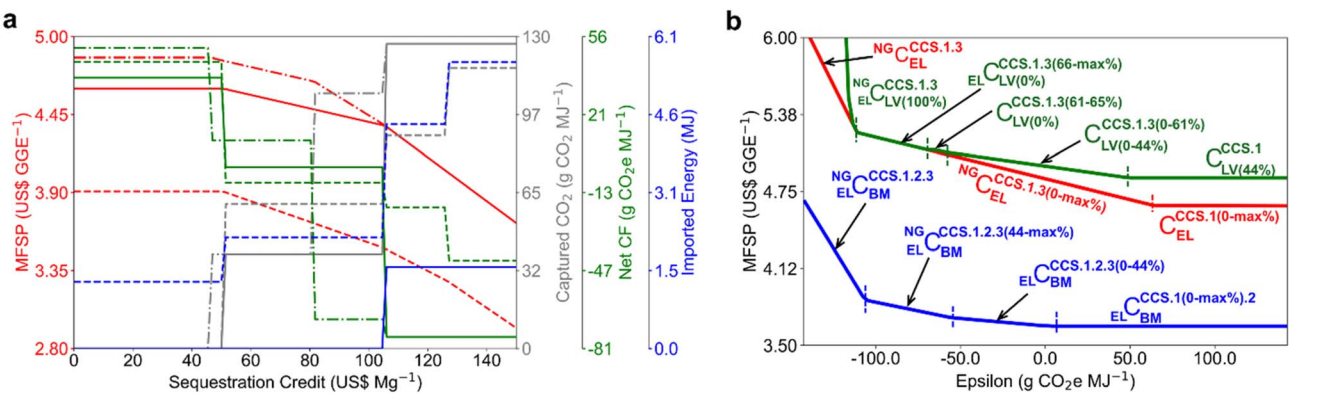

Fig. 5 Outcomes of CO_2 mitigation strategies. (a) Impact of sequestration credit on MFSP (red lines), CF (green lines), captured CO_2 (grey lines) and imported energy (blue lines). $+B_{EL}^{CCS}$ system: solid lines, $+B_{BM}^{CCS}$ system: dash-dash lines, $+B_{LV}^{CCS}$ system: dash-dot lines. Imported energy is calculated as the megajoule of electricity and natural gas purchased. (b) Impact of emission constraint on MFSP. $+B_{EL}^{CCS}$ system in red, $+B_{BM}^{CCS}$ system in blue, $+B_{LV}^{CCS}$ system in green. Values in parenthesis indicate percentage carbon captured by respective CCS options, and percentage lignin valorized.

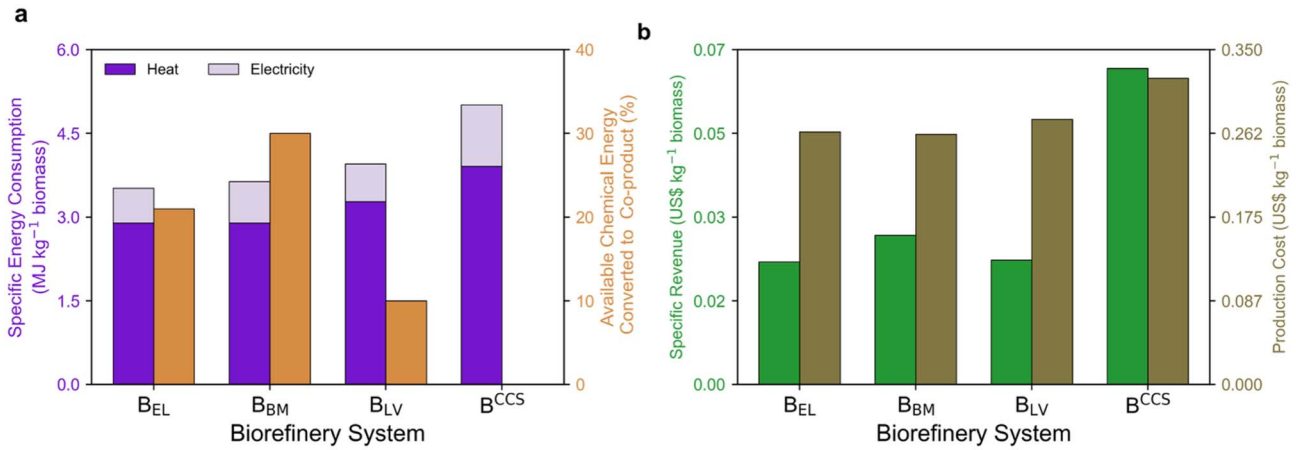

Fig. 6 Insights into co-production baseline and carbon capture systems. (a) Energy insights. Specific energy consumption, and content of co-product stream are determined by dividing the total energy (heat and electricity) use, and the energy content of the co-product by the mass of biomass feedstock, respectively. (b) Cost insights. Production cost is defined as the total production cost of all blocks in the biorefinery system divided by the biomass feedstock.

see that B^{CCS} benefits from higher revenues from CO_2 captured, which helps to offset some of its elevated production costs.

4.2 Natural gas purchase for CCS

In terms of carbon capture, a question that often arises is whether burning natural gas to capture CO_2 at the biorefinery is environmentally better than being energetically self-sufficient. In Section 3.4, we showed that more CO_2 can be captured by burning natural gas. With a calculated marginal abatement cost of US$55 per Mg CO_2, this system leads to an acceptable mitigation cost (US$50–$100 per Mg CO_2) as proposed by the Intergovernmental Panel on Climate Change (IPCC)[41] for Bioenergy with Carbon Capture and Storage (BECCS), suggesting that using natural gas for CCS in biorefineries may be both environmentally and economically favorable. However, it is important to note that burning natural gas introduces fossil-

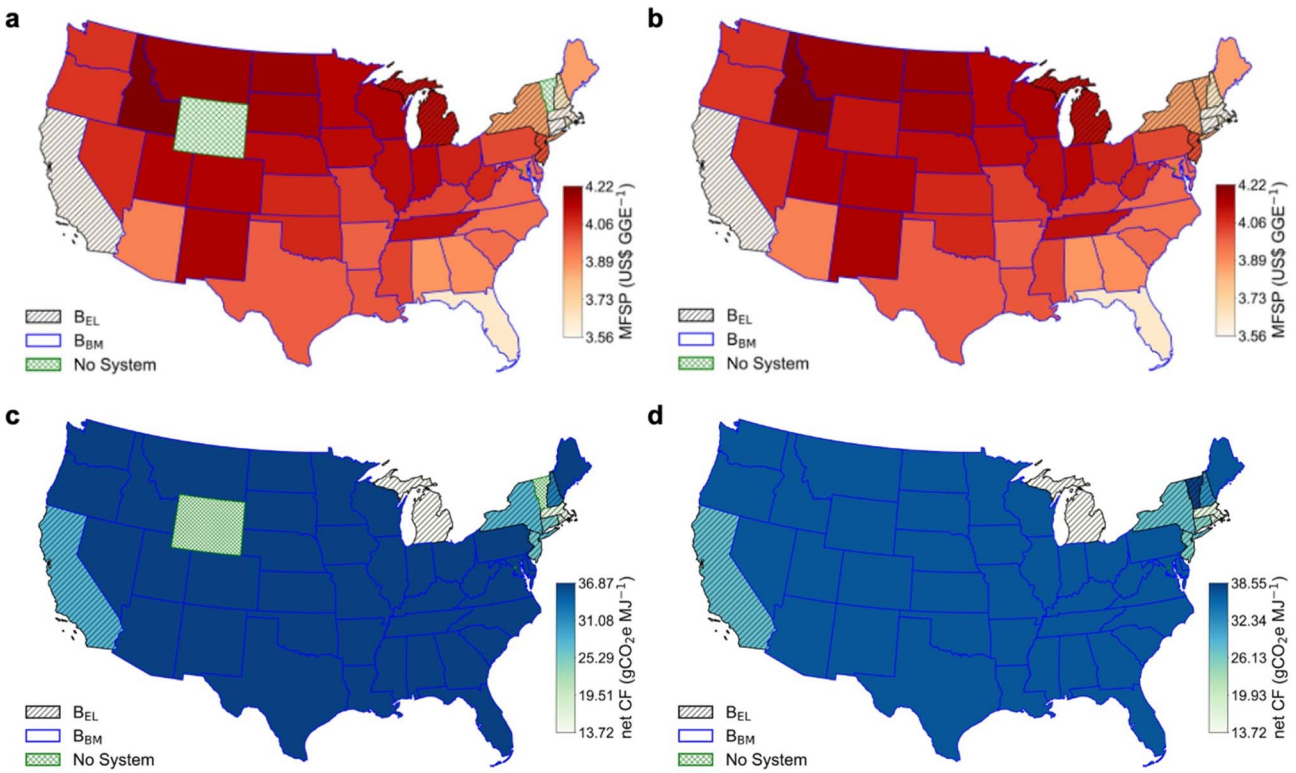

Fig. 7 State-level analysis. (a and b) MFSP of selected biorefinery system in each US state under the "near-term" and "mature-market high term" biomass availability scenarios from the 2023 Billion Ton[44] report. (c and d) CF of selected biorefinery system in each US state under the "near-term" and "mature-market high" scenarios from the 2023 Billion Ton report.

based CO_2 alongside the biogenic CO_2 from biomass in the post-combustion flue gas stream. Although this approach allows capturing more CO_2, the capturing process from the flue gas is not 100% efficient, hence a portion of the fossil-based CO_2 gets released (~27.8%), making the biorefinery *less renewable*. If the natural gas is from a renewable source, then the introduced carbon would be considered biogenic, mitigating concerns about fossil-based emissions and preserving the *renewability* of the biorefinery.

4.3 Spatial insights

We conduct a spatial analysis of potential biorefinery systems across the contiguous U.S. solving the electricity and biomethane models using 5 year average state-level co-product selling price and emission factor data. The "near-term" and "mature-market high" biomass availability scenarios in the U.S. Billion Ton (BT) Report[44] is then used to determine which states can support biorefinery deployment. For a biorefinery system to be built, we assume the state should have sufficient biomass to support a biorefinery processing 2000 dry Mg per day feedstock (which translates to an annual minimum biomass threshold of 730 000 Mg per year). From the BT report, the total biomass availability in the U.S. under the "near-term" scenario is ~628 million dry Mg per year, while that of the "mature-market high" is ~1361 million dry Mg per year.

Fig. 7 gives the MFSP (Fig. 7a and b) and net CF (Fig. 7c and d) for the selected biorefinery system in each state. We observe that the B_{EL} system is favored in the northeast (*e.g.*, Massachusetts [US$3.59 per GGE], Connecticut [US$3.57 per GGE], and New York [US$3.85 per GGE]) and west coast (California [US$3.56 per GGE]) states, due to the relatively high electricity prices, with the B_{BM} system chosen in the remaining states.

From a sustainability perspective, in states where the B_{EL} system was chosen, we observe lower CF due to higher avoided emissions, which results from high grid emission factors. For example, the B_{EL} system achieves a net CF of 16.9 g CO_2e per MJ in Massachusetts due to avoided emission of 22.9 g CO_2e per MJ resulting from a high grid emission factor of 105.7 g CO_2e per MJ (380.4 g CO_2e per kWh of electricity).

In the near-term scenario (Fig. 7a and c), there is no biorefinery system that is constructed in states like Wyoming, Vermont, and District of Columbia, as these states do not have sufficient biomass to support the required biorefinery capacity. However, in the mature-market high scenario (Fig. 7b and d), all but District of Columbia meet the required biomass threshold for biorefinery deployment.

In this study, we assumed that the average biomass truck transportation distance is 50 km, but note that increase in the average distance, will not have a significant impact in the results shown in Fig. 7 (see Fig. 8 in SI for transportation distance impact on MFSP and net CF).

5 Conclusion

This work provides a comprehensive system-level assessment of second-generation lignocellulosic biorefineries in terms of economics, CF, carbon and energy efficiency, and carbon capture potential.

We find that from an energy efficiency viewpoint, co-producing biomethane leads to the highest efficiency (58%). From an economic standpoint, co-producing biomethane results in MFSP reduction between 15% to 55% relative to co-producing electricity, due to current financial incentives for renewable fuels production. Without incentives for biomethane co-production, the MFSP reduction is ~3.5%.

From a sustainability standpoint, biorefineries with CCS present the best option. However, if we consider only the three co-production systems, co-producing electricity is the best option (net CF of 16.53 g CO_2e per MJ) and can achieve further significant reductions (~49 g CO_2e per MJ), if we consider avoided emissions from different power sources. Even with 80% decline in grid carbon intensity due to future decarbonization, co-producing electricity results in ~5% lower net carbon footprint relative to the baseline biomethane co-production. If integrated co-production and CCS are considered, then the economic viability is strongly influenced by sequestration credits. We find that credits exceeding US$106 per Mg could substantially reduce the MFSP and net CF across all systems, while fixing the credits and enforcing emission constraints could reduce emissions by a factor of 2 albeit at a cost ~14% higher.

In terms of spatial considerations, we observe that having a biorefinery with biomethane co-production might be advantageous in most U.S. states. In more than 45 states, this system is preferred, highlighting the strong economic advantage of biomethane co-production under current favorable market conditions. Conversely, in states with high electricity price such as Massachusetts, New York, and California, the electricity co-production system is preferred, further benefiting from greater avoided emissions due to high grid carbon intensities.

The findings of the paper underscore the importance of aligning financial incentives, emission reduction targets, and regional resource availability to accelerate commercial deployment. As no second-generation lignocellulosic biorefineries have yet been built in the U.S., this analysis provides insights into which system offers the most promise and under what conditions, thereby informing investment, siting, and policy decisions that can support the scale-up of sustainable biofuels. While electricity co-production has traditionally dominated system-level studies, our analysis reveals that a case for biomethane co-production also deserves further attention.

Author contributions

Conceptualization by E. A. A. and C. T. M.; data collection by E. A. A.; data analysis by E. A. A.; writing-original draft by E. A. A.; writing-review, editing, and approval of final version by E. A. A. and C. T. M.; funding acquisition by C. T. M.; supervision by C. T. M.

Conflicts of interest

The authors declare no competing interests.

Data availability

The data supporting this work has been included as part of the supplementary information (SI). Supplementary information: the data, additional figures, and the mathematical model. See DOI: https://doi.org/10.1039/d6su00050a.

Acknowledgements

This material is based upon work supported by the Great Lakes Biorefinery Research Center, US Department of Energy, Office of Science, Office of Biological and Environmental Research under award number DE-SC0018409

References

1 G. De Bhowmick, A. K. Sarmah and R. Sen, Lignocellulosic biorefinery as a model for sustainable development of biofuels and value added products, *Bioresour. Technol.*, 2018, **247**, 1144–1154.
2 B. Kumar, N. Bhardwaj, K. Agrawal, V. Chaturvedi and P. Verma, Current perspective on pretreatment technologies using lignocellulosic biomass: An emerging biorefinery concept, *Fuel Process. Technol.*, 2020, **199**, 106244.
3 S. S. Hassan, G. A. Williams and A. K. Jaiswal, Moving towards the second generation of lignocellulosic biorefineries in the EU: Drivers, challenges, and opportunities, *Renewable Sustainable Energy Rev.*, 2019, **101**, 590–599.
4 N. Singh, *et al.*, Global status of lignocellulosic biorefinery: Challenges and perspectives, *Bioresour. Technol.*, 2022, **344**, 126415.
5 S. Kim, B. E. Dale and R. Jenkins, Life cycle assessment of corn grain and corn stover in the United States, *Int. J. Life Cycle Assess.*, 2009, **14**, 160–174.
6 K. Huang, *et al.*, Greenhouse Gas Emission Mitigation Potential of Chemicals Produced from Biomass, *ACS Sustain. Chem. Eng.*, 2021, **9**, 14480–14487.
7 H. Kim, S. Kim and B. E. Dale, Biofuels, Land Use Change, and Greenhouse Gas Emissions: Some Unexplored Variables, *Environ. Sci. Technol.*, 2009, **43**, 961–967.
8 C. D. Zamuda, *et al.*, Chapter 4: Energy Supply, Delivery, and Demand, *Impacts, Risks, and Adaptation in the United States: The Fourth National Climate Assessment, Volume II*, 2018, DOI: 10.7930/NCA4.2018.CH4, https://nca2018.globalchange.gov/chapter/4/.
9 A. Patel and A. R. Shah, Integrated lignocellulosic biorefinery: Gateway for production of second generation ethanol and value added products, *J. Bioresour. Bioprod.*, 2021, **6**, 108–128.
10 D. Humbird, *et al.*, *Process Design and Economics for Biochemical Conversion of Lignocellulosic Biomass to Ethanol: Dilute-Acid Pretreatment and Enzymatic Hydrolysis of Corn Stover*, 2011, https://www.osti.gov/scitech/biblio/1013269.
11 C. H. Geissler and C. T. Maravelias, Analysis of alternative bioenergy with carbon capture strategies: present and future, *Energy Environ. Sci.*, 2022, **15**, 2679–2689.
12 P. Cheali, J. A. Posada, K. V. Gernaey and G. Sin, Upgrading of lignocellulosic biorefinery to value-added chemicals: Sustainability and economics of bioethanol-derivatives, *Biomass Bioenergy*, 2015, **75**, 282–300.
13 R. E. Davis, *et al.*, *Process Design and Economics for the Conversion of Lignocellulosic Biomass to Hydrocarbon Fuels and Coproducts: 2018 Biochemical Design Case Update; Biochemical Deconstruction and Conversion of Biomass to Fuels and Products via Integrated Biorefinery Pathways*, NREL/TP-5100-71949, 1483234, 2018, DOI: 10.2172/1483234, https://www.osti.gov/servlets/purl/1483234/.
14 R. T. L. Ng, D. H. S. Tay and D. K. S. Ng, Simultaneous Process Synthesis, Heat and Power Integration in a Sustainable Integrated Biorefinery, *Energy Fuels*, 2012, **26**, 7316–7330.
15 K. C. Surendra, C. Sawatdeenarunat, S. Shrestha, S. Sung and S. K. Khanal, Anaerobic Digestion-Based Biorefinery for Bioenergy and Biobased Products, *Ind. Biotechnol.*, 2015, **11**, 103–112.
16 J. Frigon and S. R. Guiot, Biomethane production from starch and lignocellulosic crops: a comparative review, *Biofuels, Bioprod. Biorefin.*, 2010, **4**, 447–458.
17 M. Yang, N. R. Baral, A. Anastasopoulou, H. M. Breunig and C. D. Scown, Cost and Life-Cycle Greenhouse Gas Implications of Integrating Biogas Upgrading and Carbon Capture Technologies in Cellulosic Biorefineries, *Environ. Sci. Technol.*, 2020, **54**, 12810–12819.
18 S. Sethupathy, *et al.*, Lignin valorization: Status, challenges and opportunities, *Bioresour. Technol.*, 2022, **347**, 126696.
19 R. Behling, S. Valange and G. Chatel, Heterogeneous catalytic oxidation for lignin valorization into valuable chemicals: what results? What limitations? What trends?, *Green Chem.*, 2016, **18**, 1839–1854.
20 X. Liu, *et al.*, Recent Advances in the Catalytic Depolymerization of Lignin towards Phenolic Chemicals: A Review, *ChemSusChem*, 2020, **13**, 4296–4317.
21 B. Kim, S. Misra and C. T. Maravelias, Lignocellulosic fuel and chemical co-production, *Joule*, 2023, **7**, 2403–2407.
22 X. Huang, T. I. Korányi, M. D. Boot and E. J. M. Hensen, Catalytic Depolymerization of Lignin in Supercritical Ethanol, *ChemSusChem*, 2014, **7**, 2276–2288.
23 X. Du, *et al.*, Oxidative Catalytic Fractionation and Depolymerization of Lignin in a One-Pot Single-Catalyst System, *ACS Sustain. Chem. Eng.*, 2021, **9**, 7719–7727.
24 K. Huang, P. Fasahati and C. T. Maravelias, System-Level Analysis of Lignin Valorization in Lignocellulosic Biorefineries, *iScience*, 2020, **23**, 100751.
25 A. W. Bartling, *et al.*, Techno-economic analysis and life cycle assessment of a biorefinery utilizing reductive catalytic fractionation, *Energy Environ. Sci.*, 2021, **14**, 4147–4168.
26 E. G. O'Neill, C. H. Geissler and C. T. Maravelias, Large-scale spatially explicit analysis of carbon capture at cellulosic biorefineries, *Nat. Energy*, 2024, **9**, 828–838.
27 S. V. Hanssen, *et al.*, The climate change mitigation potential of bioenergy with carbon capture and storage, *Nat. Clim. Change*, 2020, **10**, 1023–1029.

28 C. H. Geissler and C. T. Maravelias, Economic, energetic, and environmental analysis of lignocellulosic biorefineries with carbon capture, *Appl. Energy*, 2021, **302**, 117539.
29 P. Gabrielli, M. Gazzani and M. Mazzotti, The Role of Carbon Capture and Utilization, Carbon Capture and Storage, and Biomass to Enable a Net-Zero-CO_2 Emissions Chemical Industry, *Ind. Eng. Chem. Res.*, 2020, **59**, 7033–7045.
30 A. Dutta, *et al.*, *Process Design and Economics for the Conversion of Lignocellulosic Biomass to Hydrocarbon Fuels*, 2015, https://www.nrel.gov/docs/fy15osti/62455.pdf.
31 R. Davis, *et al.*, *Process Design and Economics for the Conversion of Lignocellulosic Biomass to Hydrocarbons: Dilute-Acid and Enzymatic Deconstruction of Biomass to Sugars and Catalytic Conversion of Sugars to Hydrocarbons*, NREL/TP-5100-62498, 1176746, 2015, DOI: 10.2172/1176746, https://www.osti.gov/servlets/purl/1176746/.
32 National Renewable Energy Laboratory/USLCI|LCA Collaboration Server, https://www.lcacommons.gov/lca-collaboration/National_Renewable_Energy_Laboratory/USLCI_Database_Public/datasets/Processes.
33 M. Ehsanipour, A. V. Suko and R. Bura, Fermentation of lignocellulosic sugars to acetic acid by *Moorella thermoacetica*, *J. Ind. Microbiol. Biotechnol.*, 2016, **43**, 807–816.
34 G. Merli, A. Becci, A. Amato and F. Beolchini, Acetic acid bioproduction: The technological innovation change, *Sci. Total Environ.*, 2021, **798**, 149292.
35 R. Hakawati, B. M. Smyth, G. McCullough, F. De Rosa and D. Rooney, What is the most energy efficient route for biogas utilization: Heat, electricity or transport?, *Appl. Energy*, 2017, **206**, 1076–1087.
36 A. Kiani, K. Jiang and P. Feron, Techno-Economic Assessment for CO_2 Capture From Air Using a Conventional Liquid-Based Absorption Process, *Front. Energy Res.*, 2020, **8**, 92.
37 Q. Sun, *et al.*, Selection of appropriate biogas upgrading technology-a review of biogas cleaning, upgrading and utilisation, *Renewable Sustainable Energy Rev.*, 2015, **51**, 521–532.
38 US EPA, *Renewable Energy Certificates (RECs)*, 2022, https://www.epa.gov/green-power-markets/renewable-energy-certificates-recs.
39 *Alternative Fuels Data Center: Clean Fuel Production Credit*, https://afdc.energy.gov/laws/13321.
40 US EPA, *RIN Trades and Price Information*, 2018, https://www.epa.gov/fuels-registration-reporting-and-compliance-help/rin-trades-and-price-information.
41 P. R. Shukla, J. Skea, A. Reisinger, R. Slade, R. Fradera, M. Pathak, A. A. Khourdajie, M. Belkacemi, R. v. Diemen, A. Hasija, G. Lisboa, S. Luz, J. Malley, D. McCollum, S. Some, P. Vyas, *Climate Change 2022: Mitigation of Climate Change*, IPCC, Geneva, 2022.
42 STEO Data Browser – 7c. U.S. Regional Electricity Prices to Ultimate Customers, https://www.eia.gov/outlooks/steo/data/browser/#/?v=21&f=A&s=&start=1997&end=2025&map=&linechart=~ESRCU_US&ctype=linechart&maptype=0&id=.
43 V. B. Mike, *Acetic Acid Price Index*, Businessanalytiq, 2020, https://businessanalytiq.com/procurementanalytics/index/acetic-acid-price-index/.
44 *2023 Billion-Ton Report*.